Acta Cryst E CRYSTALLOGRAPHIC COMMUNICATIONS

ISSN 2056-9890

Avutometinib

Jacob K. Salazar,[a] James A. Kaduk,[b,c]* Anja Dosen[d] and Thomas N. Blanton[d]

[a]North Central College, Department of Chemistry, 131 S. Loomis St., Naperville IL 60540 , USA, [b]North Central College, Department of Physics, 131 S. Loomis St., Naperville IL 60540 , USA, [c]Illinois Institute of Technology, Department of Chemistry, 3101 S. Dearborn St., Chicago IL 60616, USA, and [d]ICDD, 12 Campus Blvd., Newtown Square PA 19073-3273, USA. *Correspondence e-mail: kaduk@polycrystallography.com

Received 20 April 2026
Accepted 28 April 2026

Edited by F. F. Ferreira, Universidade Federal do ABC, Brazil

Keywords: powder diffraction; avutometinib; AVMAKI; Rietveld refinement; density functional theory; crystal structure.

CCDC references: 2551067; 2551068

Supporting information: this article has supporting information at journals.iucr.org/e

The crystal structure of avutometinib (systematic name: 3-{[3-fluoro-2-(methylsulfamoylamino)pyridin-4-yl]methyl}-4-methyl-7-(pyrimidin-2-yloxy)chromen-2-one), $C_{21}H_{18}FN_5O_5S$, has been solved and refined using synchrotron X-ray powder diffraction data, and optimized using density functional theory techniques. Avutometinib crystallizes in space group $P\overline{1}$ (#2). The crystal structure is composed of layers parallel to the *ab* plane. N—H···O hydrogen bonds link the layers along the *a*-axis direction. The molecule is Z-shaped.

1. Chemical context

Avutometinib (AVNAPKI) has been approved as a treatment for ovarian cancer. AVNAPKI is administered in capsule form as a co-medication with FAKZYNJA™ (defactinib tablets), for the treatment of KRAS-mutated recurrent low-grade serous ovarian cancer for patients that have previously received unsuccessful systemic therapy. The systematic name (CAS Registry Number 946128-88-7) is 3-{[3-fluoro-2-(methylsulfamoylamino)-4-pyridinyl]methyl}-4-methyl-7-pyrimidin-2-yloxychromen-2-one.

We are unaware of any published powder diffraction data for avutometinib. This work was carried out as part of a project (Kaduk *et al.*, 2014) to determine the crystal structures of large-volume commercial pharmaceuticals, and include high-quality powder diffraction data for them in the Powder Diffraction File (Kabekkodu *et al.*, 2024).

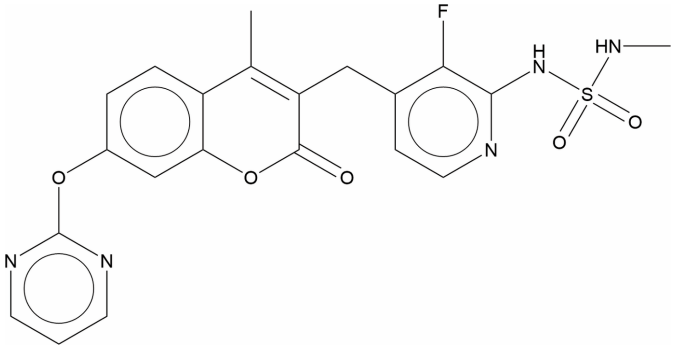

2. Structural commentary

The root-mean-square difference of the non-H atoms in the Rietveld-refined and VASP-optimized structures of avutometinib, calculated using the *Mercury* (Macrae *et al.*, 2020) CSD-Materials/Search/Crystal Packing Similarity tool is 0.059 Å (Fig. 1); the structures are essentially identical. The root-mean-square Cartesian displacement of the non-H atoms in the refined and optimized structures, calculated using the

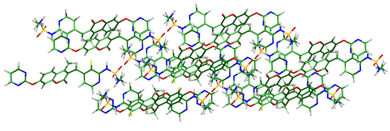

Table 1
Hydrogen-bond geometry (Å, °).

D—H···A	D—H	H···A	D···A	D—H···A	Mulliken overlap	H-bond energy
N8—H44···O4^{i}	1.04	1.95	2.961	165	0.054	5.4
N10—H45···O7^{ii}	1.03	2.22	3.223	163	0.026	3.7
N10—H45···N9	1.03	2.49	2.977	108	0.011	–
C24—H41···O6^{iii}	1.09	2.42	3.183	126	0.011	–
C33—H51···O6^{iv}	1.09	2.35	3.170	131	0.015	–
C21—H39···N11^{i}	1.09	2.80	3.882	170	0.012	–
C31—H49···N10^{iv}	1.09	2.82	3.777	145	0.011	–

Symmetry codes: (i) $x-1, y, z$; (ii) $-x, -y, 1-z$; (iii) $x+1, y, z$; (iv) $x+2, y, z-1$.

Mercury Calculate/Molecule Overlay tool, is 0.053 Å (Fig. 2). The agreements are within the normal range for correct structures (van de Streek & Neumann, 2014). The asymmetric unit is illustrated in Fig. 3. The remaining discussion will emphasize the VASP-optimized structure.

All of the bond distances, bond angles, and torsion angles fall within the normal ranges indicated by a *Mercury* Mogul Geometry check (Macrae *et al.*, 2020). Only the S1—N8 bond of 1.682 Å [average = 1.628 (17); *Z*-score = 3.1] is flagged as unusual. The unusual S—N bond distance is an example of a known feature of DFT calculations: too-long S—N bonds in the DFT optimization of sulfonamides have been observed (Kaduk *et al.*, 2025; Vibha *et al.*, 2023; Whitfield, 2025).

Quantum chemical geometry optimization of the isolated avutometinib molecule (DFT/B3LYP/6-31G*/water) using *Spartan '24* (Wavefunction, 2025) indicated that the observed conformation is 5.7 kcal mol^{-1} higher in energy than a local minimum, which has a very similar conformation. The global minimum-energy conformation is 79.9 kcal mol^{-1} lower in energy, but is folded on itself to make intramolecular hydrogen bonds. Intermolecular interactions are thus important in determining the observed solid-state conformation.

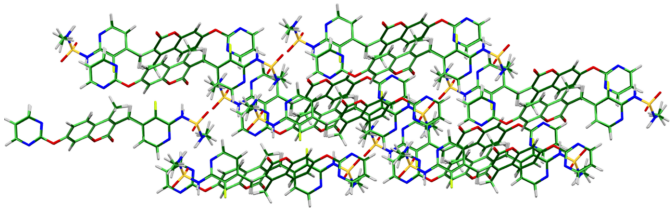

Figure 1
Comparison of the Rietveld-refined (colored by atom type) and VASP-optimized (pale green) structures of avutometinib, calculated using the *Mercury* CSD-Materials/Search/Crystal Packing Similarity tool. The root-mean-square Cartesian displacement is 0.059 Å. Image generated using *Mercury* (Macrae *et al.*, 2020).

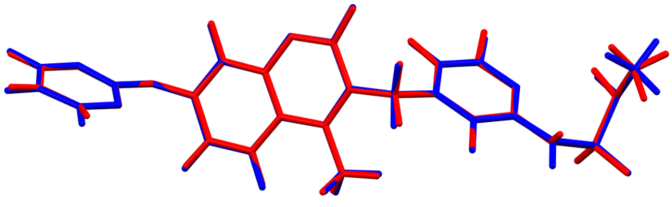

Figure 2
Comparison of the refined structure of avutometinib (red) to the VASP-optimized structure (blue). The comparison was generated using the *Mercury* Calculate/Molecule Overlay tool; the r.m.s. difference is 0.053 Å. Image generated using *Mercury* (Macrae *et al.*, 2020).

3. Supramolecular features

The crystal structure (Fig. 4) is composed of layers lying parallel to the *ab* plane. Hydrogen bonds link the layers along the *b*-axis direction (Table 1). The molecule is Z-shaped. The mean plane of the pyridine ring near the sulfonamide group is approximately (011), the mean plane of the 2*H*-chromen-2-one ring system is approximately (01$\bar{1}$), and the mean plane of the pyrimidine ring is approximately (123). The *Mercury* Aromatics Analyser indicates one strong interaction (*d* =

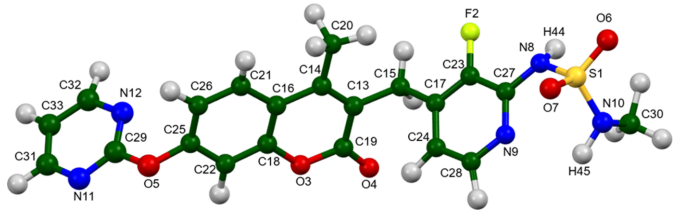

Figure 3
The asymmetric unit of avutometinib, with the atom numbering. The atoms are represented by 50% probability spheroids. Image generated using *Mercury* (Macrae *et al.*, 2020).

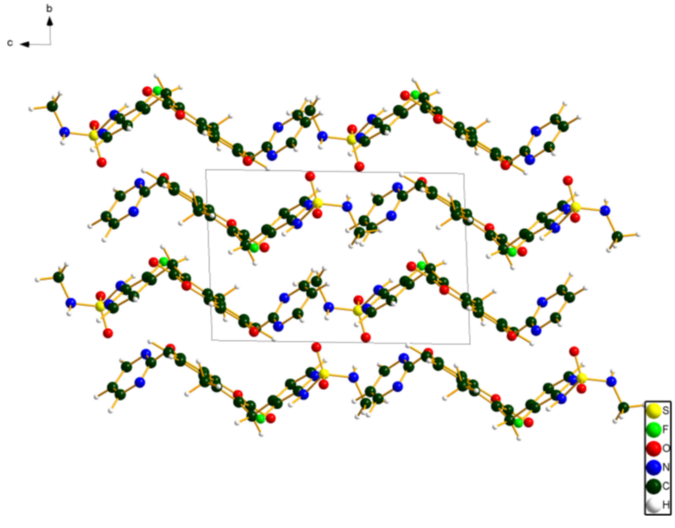

Figure 4
Crystal structure of avutometinib, viewed down the *a*-axis. Image generated using DIAMOND (Brandenburg & Putz, 2025).

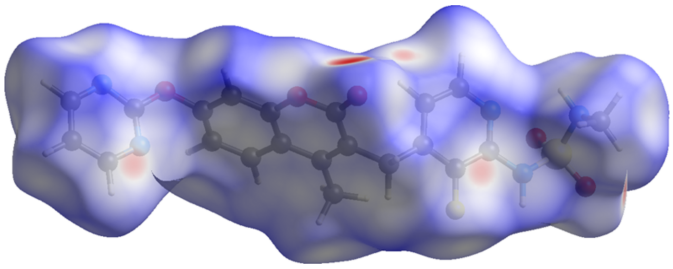

Figure 5
The Hirshfeld surface of avutometinib. Intermolecular contacts longer than the sums of the van der Waals radii are colored blue, and contacts shorter than the sums of the radii are colored red. Contacts equal to the sums of radii are white. Image generated using *CrystalExplorer* (Spackman *et al.*, 2021).

4.334 Å) between phenyl rings of the 2*H*-chromen-2-one ring system, and weaker interactions between multiple pairs of rings.

Analysis of the contributions to the total crystal energy of the structure using the Forcite module of *Materials Studio* (Dassault Systèmes, 2024) indicated that the intramolecular energy is dominated by angle distortion terms, as might be expected for a molecule containing a fused ring system. The intermolecular energy is dominated by van der Waals attractions, which in this force field based analysis include hydrogen bonds. The hydrogen bonds are better discussed using the results of the DFT calculation.

There are two classical N—H···O hydrogen bonds in the structure (Table 1), one intramolecular and one intermolecular. The energies of these hydrogen bonds were calculated using the correlation of Wheatley and Kaduk (2019). The intermolecular N8—H44···O4 hydrogen bonds link the molecules into chains along the *a*-axis direction, with graph set $C_1^1(9)$ (Etter, 1990; Bernstein *et al.*, 1995; Motherwell *et al.*, 2000). A few C—H···O and C—H···N hydrogen bonds also contribute to the cohesion of the crystal.

The volume enclosed by the Hirshfeld surface of avutometinib (Fig. 5, Hirshfeld, 1977; Spackman *et al.*, 2021) is 498.97 Å^3, 98.27% of half of the unit-cell volume. The packing density is thus typical. The only significant close contacts (red

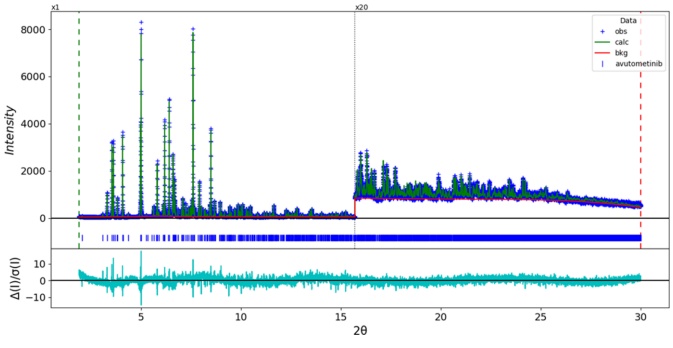

Figure 6
The Rietveld plot for avutometinib. The blue crosses represent the observed data points, and the green line is the calculated pattern. The cyan curve is the normalized error plot, and the red line is the background curve. The blue tick marks indicate the peak positions. The vertical scale has been multiplied by a factor of 20× for $2\theta > 15.7°$.

Table 2
Experimental details.

	avutometinib
Crystal data	
Chemical formula	$C_{21}H_{18}FN_5O_5S$
M_r	471.46
Crystal system, space group	Triclinic, $P\overline{1}$
Temperature (K)	295
a, *b*, *c* (Å)	8.91097 (5), 9.47933 (5), 13.24641 (9)
α, β, γ (°)	83.9821 (4), 81.7759 (3), 66.67667 (9)
V (Å^3)	1015.49 (1)
Z	2
Radiation type	Synchrotron, λ = 0.46873 Å
μ (mm^{-1})	0.02
Specimen shape, size (mm)	Cylinder, 2.0 × 1.5
Data collection	
Diffractometer	11-BM, APS
Specimen mounting	Kapton capillary
Data collection mode	Transmission
Scan method	Step
2θ values (°)	$2\theta_{min}$ = 0.510, $2\theta_{max}$ = 49.995, $2\theta_{step}$ = 0.001
Refinement	
R factors and goodness of fit	R_p = 0.058, R_{wp} = 0.072, R_{exp} = 0.043, $R(F^2)$ = 0.06083, χ^2 = 2.941
No. of parameters	136
No. of restraints	91
$(\Delta/\sigma)_{max}$	1.795

Computer programs: *GSAS-II* (Toby & Von Dreele, 2013).

in Fig. 5) involve the hydrogen bonds. The volume/non-hydrogen atom is smaller than normal, at 15.4 Å^3.

The Bravais–Friedel–Donnay–Harker (Bravais, 1866; Friedel, 1907; Donnay and Harker, 1937) algorithm suggests that we might expect lozenge morphology for avutometinib, with {001} as the major faces. A 2nd-order spherical harmonic model for preferred orientation was included. The texture index was 1.002, indicating that the preferred orientation was insignificant in this rotated capillary specimen.

4. Database survey

A reduced cell search of the Cambridge Structural Database (Groom *et al.*, 2016) yielded no hits.

5. Synthesis and crystallization

Avutometinib was a commercial reagent, purchased from Sigma (Batch #A245684-HA3), and was used as-received.

6. Refinement

Crystal data, data collection and structure refinement details are summarized in Table 2. The white powder was packed into a 1.5 mm diameter Kapton capillary, and rotated during the measurement at ∼50 Hz. The powder pattern was measured at 295 K at beam line 11-BM (Lee *et al.*, 2008; Wang *et al.*, 2008; Antao *et al.*, 2008) of the Advanced Photon Source at Argonne National Laboratory using a wavelength of

0.4687342 Å from 0.5–50° 2θ with a step size of 0.001° and a counting time of 0.1 sec/step. The high-resolution powder diffraction data were collected using twelve silicon crystal analyzers that allow for high angular resolution, high precision, and accurate peak positions. A mixture of silicon (NIST SRM 640c) and alumina (NIST SRM 676a) standards (ratio Al_2O_3:Si = 2:1 by weight) was used to calibrate the instrument and refine the monochromatic wavelength used in the experiment.

The pattern was indexed on a high-quality primitive triclinic unit cell with a = 8.91271, b = 9.47911, c = 13.29736 Å, α = 83.91, β = 81.66, γ = 66.67°, V = 1019.23 Å^3, and Z = 2 using *JADE Pro* (MDI, 2025). The space group was assumed to be $P\overline{1}$, which was confirmed by successful solution and refinement of the structure.

The molecular structure of avutometinib was downloaded from PubChem (Kim *et al.*, 2023) as Conformer3D_COMPOUND_CID_16719221.sdf. It was converted to a *.mol2 file using *Mercury* (Macrae *et al.*, 2020), and to a Fenske–Hall *Z*-matrix using *OpenBabel* (O'Boyle *et al.*, 2011). The structure was solved using parallel tempering techniques as implemented in *FOX* (Favre-Nicolin & Černý, 2002).

Rietveld refinement was carried out using *GSAS-II* (Toby & Von Dreele, 2013). Only the 1.9–30.0° portion of the pattern was included in the refinements (d_{min} = 0.905 Å). The μR value was fixed at 0.02, calculated using the 11-BM web site (https://11bm.xray.aps.anl.gov/absorb/). All non-H bond distances and angles were subjected to restraints, based on a *Mercury*/Mogul Geometry Check (Sykes *et al.*, 2011; Bruno *et al.*, 2004). The Mogul average and standard deviation for each quantity were used as the restraint parameters. The aromatic rings were restrained to be planar. The restraints contributed 3.7% to the overall χ^2. The hydrogen atoms were included in calculated positions, which were recalculated during the refinement using *Materials Studio* (Dassault Systèmes, 2024). The U_{iso} values were grouped by chemical similarity. The peak profiles were described using the generalized microstrain model (Stephens, 1999). The background was modeled using a six-term shifted Chebyshev polynomial, with a peak at 5.87° 2θ to model the scattering from the Kapton capillary and any amorphous component of the sample.

The final refinement of 136 variables using 28,101 observations and 91 restraints yielded the residuals R_{wp} = 0.0737 and GOF = 1.72. The largest peak (1.08 Å from C27) and hole (1.82 Å from N8) in the difference-Fourier map are 0.49 (11) and −0.46 (11) eÅ^{-3}, respectively. The final Rietveld plot is shown in Fig. 6. The largest features in the normalized error plot are in the positions and shapes of some of the strong low-angle peaks, and may indicate a change of the specimen during the measurement.

The crystal structure of avutometinib was optimized (fixed experimental unit cell) with density functional theory techniques using *VASP* (Kresse & Furthmüller, 1996) through the *MedeA* graphical interface (Materials Design, 2024). The calculation was carried out on 32 cores of a 144-core (768 Gb memory) HPE Superdome Flex 280 Linux server at North Central College. The calculation used the GGA-PBE functional, a plane wave cutoff energy of 400.0 eV, and a k-point spacing of 0.5 Å^{-1} leading to a 2 × 2 × 1 mesh, and took ∼1.1 h. Single-point density functional theory calculations (fixed experimental cell) and population analysis were carried out using *CRYSTAL23* (Erba *et al.*, 2023). (fixed experimental cell) and population analysis were carried out using *CRYSTAL17* (Dovesi *et al.*, 2018). The basis sets for the H, C, N and O atoms in the calculation were those of Gatti *et al.* (1994), and those for F and S were those of Peintinger *et al.* (2013). The calculations were run on a 3.5 GHz PC using 8 k-points and the B3LYP functional, and took ∼2.7 h. The powder pattern has been submitted to ICDD for inclusion in the Powder Diffraction File.

Acknowledgements

Use of the Advanced Photon Source at Argonne National Laboratory was supported by the U. S. Department of Energy, Office of Science, Office of Basic Energy Sciences, under Contract No. DE-AC02-06CH11357. We thank Saul Lapidus for his assistance in the data collection. We also thank the ICDD team – Megan Rost, Steve Trimble, and Dave Bohnenberger – for their contribution to research, sample preparation, and in-house XRD data collection and verification.

Funding information

Funding for this research was provided by: International Centre for Diffraction Data (grant No. 09-03).

References

Antao, S. M., Hassan, I., Wang, J., Lee, P. L. & Toby, B. H. (2008). *Can. Mineral.* **46**, 1501–1509.
Bernstein, J., Davis, R. E., Shimoni, L. & Chang, N. L. (1995). *Angew. Chem. Int. Ed. Engl.* **34**, 1555–1573.
K. Brandenburg, K. & Putz, H. (2025). *DIAMOND V 5.1.1*. Crystal Impact, Bonn, Germany.
Bravais, A. (1866). *Etudes Cristallographiques.* Paris: Gauthier Villars.
Bruno, I. J., Cole, J. C., Kessler, M., Luo, J., Motherwell, W. D. S., Purkis, L. H., Smith, B. R., Taylor, R., Cooper, R. I., Harris, S. E. & Orpen, A. G. (2004). *J. Chem. Inf. Comput. Sci.* **44**, 2133–2144.
Dassault Systèmes. (2024). *BIOVIA Materials Studio 2025*. BIOVIA, San Diego, CA
Donnay, J. D. H. & Harker, D. (1937). *Am. Mineral.* **22**, 446-467.
Dovesi, R., Erba, A., Orlando, R., Zicovich-Wilson, C. M., Civalleri, B., Maschio, L., Rérat, M., Casassa, S., Baima, J., Salustro, S. & Kirtman, B. (2018). *WIREs Comput. Mol. Sci.* **8**, e1360.
Erba, A., Desmarais, J. K., Casassa, S., Civalleri, B., Donà, L., Bush, I. J., Searle, B., Maschio, L., Edith-Daga, L., Cossard, A., Ribaldone, C., Ascrizzi, E., Marana, N. L., Flament, J.-P. & Kirtman, B. (2023). *J. Chem. Theory Comput.* **19**, 6891–6932.
Etter, M. C. (1990). *Acc. Chem. Res.* **23**, 120–126.
Favre-Nicolin, V. & Černý, R. (2002). *J. Appl. Cryst.* **35**, 734–743.
Friedel, G. (1907). *Bull. Soc. Française Minéral.* **30**, 326–455.
Gatti, C., Saunders, V. R. & Roetti, C. (1994). *J. Chem. Phys.* **101**, 10686–10696.
Groom, C. R., Bruno, I. J., Lightfoot, M. P. & Ward, S. C. (2016). *Acta Cryst.* B**72**, 171–179.

Hirshfeld, F. L. (1977). *Theor. Chim. Acta* **44**, 129–138.
Kabekkodu, S., Dosen, A. & Blanton, T. N. (2024). *Powder Diffr.* **39**, 47–59.
Kaduk, J. A., Crowder, C. E., Zhong, K., Fawcett, T. G. & Suchomel, M. R. (2014). *Powder Diffr.* **29**, 269–273.
Kaduk, J. A., Dosen, A. & Blanton, T. N. (2025). *Powder Diffr.* **40**, 168–174.
Kim, S., Chen, J., Cheng, T., Gindulyte, A., He, J., He, S., Li, Q., Shoemaker, B. A., Thiessen, P. A., Yu, B., Zaslavsky, L., Zhang, J. & Bolton, E. E. (2023). *Nucleic Acids Res.* **51**, D1373–D1380.
Kresse, G. & Furthmüller, J. (1996). *Comput. Mater. Sci.* **6**, 15–50.
Lee, P. L., Shu, D., Ramanathan, M., Preissner, C., Wang, J., Beno, M. A., Von Dreele, R. B., Ribaud, L., Kurtz, C., Antao, S. M., Jiao, X. & Toby, B. H. (2008). *J. Synchrotron Rad.* **15**, 427–432.
Macrae, C. F., Sovago, I., Cottrell, S. J., Galek, P. T. A., McCabe, P., Pidcock, E., Platings, M., Shields, G. P., Stevens, J. S., Towler, M. & Wood, P. A. (2020). *J. Appl. Cryst.* **53**, 226–235.
Materials Design. (2024). *MedeA 3.7.2*. Materials Design Inc., San Diego, USA.
MDI. (2025). *JADE Pro version 9.3*. Materials Data, Livermore, USA.
Motherwell, W. D. S., Shields, G. P. & Allen, F. H. (2000). *Acta Cryst.* B**56**, 857–871.
O'Boyle, N. M., Banck, M., James, C. A., Morley, C., Vandermeersch, T. & Hutchison, G. R. (2011). *J. Cheminform* **3**, 33.
Peintinger, M. F., Oliveira, D. V. & Bredow, T. (2013). *J. Comput. Chem.* **34**, 451–459.
Spackman, P. R., Turner, M. J., McKinnon, J. J., Wolff, S. K., Grimwood, D. J., Jayatilaka, D. & Spackman, M. A. (2021). *J. Appl. Cryst.* **54**, 1006–1011.
Stephens, P. W. (1999). *J. Appl. Cryst.* **32**, 281–289.
Streek, J. van de & Neumann, M. A. (2014). *Acta Cryst.* B**70**, 1020–1032.
Sykes, R. A., McCabe, P., Allen, F. H., Battle, G. M., Bruno, I. J. & Wood, P. A. (2011). *J. Appl. Cryst.* **44**, 882–886.
Toby, B. H. & Von Dreele, R. B. (2013). *J. Appl. Cryst.* **46**, 544–549.
Vibha, K., Prachality, N. C., Reddy, R. A., Ravikantha, M. N. & Thipperudrappa, J. (2023). *Chem. Phys. Impact* **6**, 100147.
Wang, J., Toby, B. H., Lee, P. L., Ribaud, L., Antao, S. M., Kurtz, C., Ramanathan, M., Von Dreele, R. B. & Beno, M. A. (2008). *Rev. Sci. Instrum.* **79**, 085105.
Wavefunction (2025). *Spartan '24. V. 1.3.1.* Wavefunction Inc., Irvine, USA.
Wheatley, A. M. & Kaduk, J. A. (2019). *Powder Diffr.* **34**, 35–43.
Whitfield, P. S. (2025). 18th Pharmaceutical Powder X-ray Diffraction Symposium, Cambridge UK.

supporting information

Acta Cryst. (2026). E**82**, 651-655 [https://doi.org/10.1107/S2056989026004482]

Avutometinib

Jacob K. Salazar, James A. Kaduk, Anja Dosen and Thomas N. Blanton

Computing details

3-{[3-Fluoro-2-(methylsulfamoylamino)pyridin-4-yl]methyl}-4-methyl-7-(pyrimidin-2-yloxy)chromen-2-one (avutometinib)

Crystal data

$C_{21}H_{18}FN_5O_5S$
M_r = 471.46
Triclinic, $P\overline{1}$
a = 8.91097 (5) Å
b = 9.47933 (5) Å
c = 13.24641 (9) Å
α = 83.9821 (4)°
β = 81.7759 (3)°
γ = 66.67667 (9)°
V = 1015.49 (1) Å^3
Z = 2
D_x = 1.542 Mg m^{-3}
Synchrotron radiation, λ = 0.46873 Å
μ = 0.02 mm^{-1}
T = 295 K
cylinder, 2.0 × 1.5 mm

Data collection

11-BM, APS diffractometer
Specimen mounting: Kapton capillary
Data collection mode: transmission
Scan method: step
$2\theta_{min}$ = 0.510°, $2\theta_{max}$ = 49.995°, $2\theta_{step}$ = 0.001°

Refinement

Least-squares matrix: full
R_p = 0.058
R_{wp} = 0.072
R_{exp} = 0.043
$R(F^2)$ = 0.06083
49486 data points
Profile function: Finger-Cox-Jephcoat function parameters U, V, W, X, Y, SH/L: peak variance(Gauss) = Utan(Th)^2+Vtan(Th)+W: peak HW(Lorentz) = X/cos(Th)+Ytan(Th); SH/L = S/L+H/L U, V, W in (centideg)^2, X & Y in centideg 1.163, -0.126, 0.063, 0.000, 0.000, 0.002,
136 parameters
91 restraints
27 constraints
Weighting scheme based on measured s.u.'s
$(\Delta/\sigma)_{max}$ = 1.795
Background function: Background function: "chebyschev-1" function with 6 terms: 39.70(6), -8.12(8), -5.86(7), 0.45(8), -3.44(7), -0.18(6), Background peak parameters: pos, int, sig, gam: 5.871(8), 5.48(8)e3, 4.80(12)e3, 0.100,
Preferred orientation correction: Simple spherical harmonic correction Order = 2 Coefficients: 0:0:C(2,-2) = 0.0570; 0:0:C(2,-1) = -0.0160; 0:0:C(2,0) = -0.0620; 0:0:C(2,1) = -0.0340; 0:0:C(2,2) = 0.0470

Fractional atomic coordinates and isotropic or equivalent isotropic displacement parameters (Å^2)

	x	*y*	*z*	U_{iso}*/U_{eq}
S1	−0.24645 (18)	0.18626 (18)	0.42794 (12)	0.0421 (6)*
F2	−0.0709 (3)	0.4497 (3)	0.18047 (17)	0.0346 (5)*
O3	0.7085 (3)	0.3231 (4)	0.0934 (2)	0.0365 (4)*

O4	0.5286 (3)	0.4613 (4)	0.2123 (2)	0.0365 (4)*
O5	1.1225 (4)	0.0538 (4)	−0.1592 (2)	0.0466 (7)*
O6	−0.4215 (3)	0.2499 (3)	0.4256 (2)	0.0429 (9)*
O7	−0.1487 (3)	0.0326 (3)	0.4038 (2)	0.0429 (9)*
N8	−0.1842 (3)	0.2993 (4)	0.3460 (2)	0.0346 (5)*
N9	0.0824 (4)	0.1928 (4)	0.3953 (2)	0.0346 (5)*
N10	−0.2097 (4)	0.2032 (3)	0.5409 (2)	0.0407 (13)*
N11	1.3412 (4)	0.0840 (4)	−0.2574 (3)	0.0466 (7)*
N12	1.0651 (3)	0.2462 (5)	−0.2842 (3)	0.0466 (7)*
C13	0.4224 (3)	0.3609 (5)	0.0948 (3)	0.0365 (4)*
C14	0.4605 (3)	0.2760 (5)	0.0115 (3)	0.0365 (4)*
C15	0.2494 (3)	0.4418 (3)	0.1438 (3)	0.0346 (5)*
C16	0.6307 (3)	0.2123 (5)	−0.0350 (3)	0.0365 (4)*
C17	0.1945 (3)	0.3467 (5)	0.2286 (3)	0.0346 (5)*
C18	0.7480 (3)	0.2434 (6)	0.0065 (3)	0.0365 (4)*
C19	0.5500 (3)	0.3855 (5)	0.1392 (3)	0.0365 (4)*
C20	0.3333 (4)	0.2424 (5)	−0.0335 (3)	0.0365 (4)*
C21	0.6807 (4)	0.1290 (6)	−0.1232 (3)	0.0365 (4)*
C22	0.9097 (4)	0.1913 (5)	−0.0337 (3)	0.0365 (4)*
C23	0.0353 (3)	0.3584 (5)	0.2461 (3)	0.0346 (5)*
C24	0.3001 (3)	0.2514 (5)	0.2970 (3)	0.0346 (5)*
C25	0.9547 (4)	0.1156 (5)	−0.1231 (3)	0.0365 (4)*
C26	0.8430 (4)	0.0789 (6)	−0.1659 (3)	0.0365 (4)*
C27	−0.0221 (3)	0.2850 (5)	0.3307 (3)	0.0346 (5)*
C28	0.2402 (4)	0.1795 (5)	0.3777 (3)	0.0346 (5)*
C29	1.1788 (4)	0.1324 (5)	−0.2371 (3)	0.0466 (7)*
C30	−0.2810 (6)	0.3515 (4)	0.5876 (3)	0.0407 (13)*
C31	1.3927 (3)	0.1638 (6)	−0.3335 (4)	0.0466 (7)*
C32	1.1255 (5)	0.3191 (5)	−0.3622 (3)	0.0466 (7)*
C33	1.2907 (6)	0.2808 (6)	−0.3893 (3)	0.0466 (7)*
H34	0.23891	0.55099	0.17829	0.0415*
H35	0.16192	0.47507	0.08245	0.0415*
H36	0.20524	0.32410	−0.00294	0.0438*
H37	0.34758	0.11858	−0.01145	0.0438*
H38	0.35062	0.25904	−0.12025	0.0438*
H39	0.58774	0.10215	−0.16017	0.0438*
H40	1.00374	0.21103	0.00682	0.0438*
H41	0.43511	0.23367	0.28555	0.0437*
H42	0.88436	0.00750	−0.23630	0.0438*
H43	0.33257	0.10460	0.43208	0.0437*
H44	−0.26680	0.38460	0.30380	0.0437*
H45	−0.24990	0.13320	0.59250	0.0489*
H46	−0.17896	0.37943	0.61243	0.0489*
H47	−0.37075	0.34632	0.65705	0.0489*
H48	−0.34902	0.44468	0.52986	0.0489*
H49	1.52990	0.13446	−0.35462	0.0559*
H50	1.03796	0.41730	−0.40887	0.0559*
H51	1.34347	0.34168	−0.45476	0.0559*

Geometric parameters (Å, º)

S1—O6	1.4366 (19)	C22—C25	1.376 (2)
S1—O7	1.413 (2)	C22—H40	1.140 (3)
S1—N8	1.640 (2)	C23—F2	1.353 (2)
S1—N10	1.6130 (18)	C23—C17	1.365 (2)
F2—C23	1.353 (2)	C23—C27	1.3987 (18)
O3—C18	1.369 (2)	C24—C17	1.386 (2)
O3—C19	1.3724 (18)	C24—C28	1.365 (3)
O4—C19	1.213 (3)	C24—H41	1.136 (2)
O5—C25	1.403 (3)	C25—O5	1.403 (3)
O5—C29	1.363 (3)	C25—C22	1.376 (2)
O6—S1	1.4366 (19)	C25—C26	1.383 (3)
O7—S1	1.413 (2)	C26—C21	1.384 (3)
N8—S1	1.640 (2)	C26—C25	1.383 (3)
N8—C27	1.383 (2)	C26—H42	1.140 (3)
N8—H44	1.030 (3)	C27—N8	1.383 (2)
N9—C27	1.338 (2)	C27—N9	1.338 (2)
N9—C28	1.349 (3)	C27—C23	1.3987 (18)
N10—S1	1.6130 (18)	C28—N9	1.349 (3)
N10—C30	1.459 (2)	C28—C24	1.365 (3)
N10—H45	1.029 (3)	C28—H43	1.140 (3)
N11—C29	1.3283 (17)	C29—O5	1.363 (3)
N11—C31	1.335 (3)	C29—N11	1.3283 (17)
N12—C29	1.3248 (17)	C29—N12	1.3248 (17)
N12—C32	1.349 (3)	C30—N10	1.459 (2)
C13—C14	1.357 (2)	C30—H46	1.140 (4)
C13—C15	1.506 (2)	C30—H47	1.140 (4)
C13—C19	1.457 (3)	C30—H48	1.140 (5)
C14—C13	1.357 (2)	C31—N11	1.335 (3)
C14—C16	1.459 (2)	C31—C33	1.351 (3)
C14—C20	1.504 (2)	C31—H49	1.140 (3)
C15—C13	1.506 (2)	C32—N12	1.349 (3)
C15—C17	1.515 (2)	C32—C33	1.371 (3)
C15—H34	1.140 (3)	C32—H50	1.140 (3)
C15—H35	1.140 (3)	C33—C31	1.351 (3)
C16—C14	1.459 (2)	C33—C32	1.371 (3)
C16—C18	1.388 (2)	C33—H51	1.140 (3)
C16—C21	1.397 (2)	H34—C15	1.140 (3)
C17—C15	1.515 (2)	H35—C15	1.140 (3)
C17—C23	1.365 (2)	H36—C20	1.140 (4)
C17—C24	1.386 (2)	H37—C20	1.140 (5)
C18—O3	1.369 (2)	H38—C20	1.140 (4)
C18—C16	1.388 (2)	H39—C21	1.140 (3)
C18—C22	1.369 (3)	H40—C22	1.140 (3)
C19—O3	1.3724 (18)	H41—C24	1.136 (2)
C19—O4	1.213 (3)	H42—C26	1.140 (3)
C19—C13	1.457 (3)	H43—C28	1.140 (3)

C20—C14	1.504 (2)	H44—N8	1.030 (3)
C20—H36	1.140 (4)	H45—N10	1.029 (3)
C20—H37	1.140 (5)	H46—C30	1.140 (4)
C20—H38	1.140 (4)	H47—C30	1.140 (4)
C21—C16	1.397 (2)	H48—C30	1.140 (5)
C21—C26	1.384 (3)	H49—C31	1.140 (3)
C21—H39	1.140 (3)	H50—C32	1.140 (3)
C22—C18	1.369 (3)	H51—C33	1.140 (3)

O6—S1—O7	121.73 (17)	H36—C20—H38	109.5 (4)
O6—S1—N8	103.46 (18)	H37—C20—H38	109.5 (3)
O7—S1—N8	107.88 (19)	C16—C21—C26	120.21 (16)
O6—S1—N10	108.15 (18)	C16—C21—H39	120.0 (2)
O7—S1—N10	105.89 (17)	C26—C21—H39	119.8 (3)
N8—S1—N10	109.38 (17)	C18—C22—C25	118.60 (17)
C18—O3—C19	122.01 (12)	C18—C22—H40	120.0 (2)
C25—O5—C29	118.2 (3)	C25—C22—H40	121.4 (2)
S1—N8—C27	122.28 (18)	F2—C23—C17	117.97 (14)
S1—N8—H44	120.1 (2)	F2—C23—C27	119.41 (14)
C27—N8—H44	117.7 (2)	C17—C23—C27	122.57 (11)
C27—N9—C28	117.74 (16)	C17—C24—C28	119.33 (12)
S1—N10—C30	121.0 (2)	C17—C24—H41	120.0 (2)
S1—N10—H45	109.5 (2)	C28—C24—H41	120.7 (3)
C30—N10—H45	103.5 (3)	O5—C25—C22	117.7 (3)
C29—N11—C31	114.62 (10)	O5—C25—C26	120.7 (3)
C29—N12—C32	114.34 (10)	C22—C25—C26	120.73 (16)
C14—C13—C15	123.60 (17)	C21—C26—C25	119.86 (16)
C14—C13—C19	120.69 (10)	C21—C26—H42	120.1 (3)
C15—C13—C19	115.64 (17)	C25—C26—H42	120.1 (3)
C13—C14—C16	119.32 (10)	N8—C27—N9	119.01 (15)
C13—C14—C20	122.09 (13)	N8—C27—C23	121.04 (14)
C16—C14—C20	118.57 (13)	N9—C27—C23	119.86 (10)
C13—C15—C17	114.1 (2)	N9—C28—C24	124.01 (15)
C13—C15—H34	109.5 (2)	N9—C28—H43	120.0 (3)
C17—C15—H34	107.1 (3)	C24—C28—H43	116.0 (3)
C13—C15—H35	108.7 (3)	O5—C29—N11	116.0 (3)
C17—C15—H35	108.7 (2)	O5—C29—N12	116.1 (3)
H34—C15—H35	108.7 (2)	N11—C29—N12	127.94 (13)
C14—C16—C18	118.57 (10)	N10—C30—H46	109.4 (4)
C14—C16—C21	123.50 (15)	N10—C30—H47	109.5 (4)
C18—C16—C21	117.81 (14)	H46—C30—H47	109.5 (3)
C15—C17—C23	121.66 (17)	N10—C30—H48	109.4 (3)
C15—C17—C24	121.79 (17)	H46—C30—H48	109.5 (4)
C23—C17—C24	116.40 (10)	H47—C30—H48	109.5 (4)
O3—C18—C16	121.12 (11)	N11—C31—C33	123.81 (16)
O3—C18—C22	116.32 (15)	N11—C31—H49	120.0 (4)
C16—C18—C22	122.50 (15)	C33—C31—H49	116.2 (4)
O3—C19—O4	115.99 (17)	N12—C32—C33	122.95 (16)

O3—C19—C13	118.12 (12)	N12—C32—H50	120.0 (4)
O4—C19—C13	125.85 (17)	C33—C32—H50	117.1 (4)
C14—C20—H36	109.5 (2)	C31—C33—C32	116.29 (17)
C14—C20—H37	109.5 (4)	C31—C33—H51	120.0 (4)
H36—C20—H37	109.5 (3)	C32—C33—H51	123.7 (4)
C14—C20—H38	109.5 (3)		

(avutometinib_VASP)

Crystal data

$C_{21}H_{18}FN_5O_5S$	$\alpha = 83.98°$
$M_r = 471.46$	$\beta = 81.78°$
Triclinic, $P\overline{1}$	$\gamma = 66.68°$
$a = 8.91097$ Å	$V = 1015.53$ Å^3
$b = 9.47933$ Å	$Z = 2$
$c = 13.24641$ Å	

Data collection

$h = \rightarrow$	$l = \rightarrow$
$k = \rightarrow$	

Fractional atomic coordinates and isotropic or equivalent isotropic displacement parameters (Å^2)

	x	y	z	B_{iso}*/B_{eq}
S1	−0.24757	0.18753	0.42895	
F2	−0.07477	0.45568	0.17671	
O3	0.71646	0.31732	0.09192	
O4	0.53929	0.45121	0.21599	
O5	1.12701	0.05321	−0.16336	
O6	−0.42292	0.24813	0.42629	
O7	−0.14823	0.03113	0.40340	
N8	−0.19006	0.30945	0.34680	
N9	0.07524	0.19945	0.39447	
N10	−0.21091	0.20419	0.54292	
N11	1.34192	0.08760	−0.25877	
N12	1.06472	0.25390	−0.28664	
C13	0.42895	0.35914	0.09446	
C14	0.46617	0.27131	0.01093	
C15	0.25568	0.44005	0.14351	
C16	0.63371	0.20853	−0.03693	
C17	0.19668	0.34780	0.22776	
C18	0.75384	0.23729	0.00578	
C19	0.55739	0.38083	0.13895	
C20	0.33632	0.24377	−0.03426	
C21	0.68522	0.12449	−0.12629	
C22	0.91658	0.18843	−0.03742	
C23	0.03348	0.36349	0.24311	
C24	0.30019	0.24992	0.29808	
C25	0.96096	0.10896	−0.12596	
C26	0.84706	0.07495	−0.17096	

C27	−0.02552	0.28926	0.32727
C28	0.23404	0.17983	0.37918
C29	1.17844	0.13683	−0.24060
C30	−0.28532	0.35499	0.58704
C31	1.39657	0.16416	−0.33617
C32	1.12400	0.32658	−0.36442
C33	1.29130	0.28551	−0.39322
H34	0.24832	0.54394	0.17773
H35	0.16996	0.48068	0.08520
H36	0.22340	0.27002	0.01837
H37	0.37818	0.12413	−0.05544
H38	0.30606	0.31650	−0.10496
H39	0.59597	0.09911	−0.16153
H40	1.00632	0.21209	−0.00181
H41	0.42946	0.23167	0.29139
H42	0.88621	0.01237	−0.24077
H43	0.31035	0.10618	0.43672
H44	−0.27345	0.36968	0.29517
H45	−0.08805	0.14370	0.55085
H46	−0.22639	0.43396	0.55260
H47	−0.27350	0.33849	0.66903
H48	−0.41643	0.40770	0.57712
H49	1.52997	0.12683	−0.35303
H50	1.03244	0.42144	−0.40429
H51	1.33943	0.34281	−0.45717

Hydrogen-bond geometry (Å, º)

D—H···*A*	*D*—H	H···*A*	*D*···*A*	*D*—H···*A*
N8—H44···O4^{i}	1.036	1.947	2.961	165.2
N10—H45···O7^{ii}	1.030	2.222	3.223	163.4
N10—H45···N9	1.030	2.491	2.977	108.1
C24—H41···O6^{iii}	1.087	2.417	3.183	126.3
C33—H51···O6^{iv}	1.087	2.350	3.170	130.9
C21—H39···N11^{i}	1.091	2.803	3.882	170.3
C31—H49···N10^{iv}	1.094	2.826	3.777	145.3

Symmetry codes: (i) *x*−1, *y*, *z*; (ii) −*x*, −*y*, −*z*+1; (iii) *x*+1, *y*, *z*; (iv) *x*+2, *y*, *z*−1.